[12] Nachtsheim, P. R., "Stability of Crosshatched Wave Patterns in Thin Liquid Films Adjacent to Supersonic Streams," *The Physics of Fluids*, Vol. 13, 1970, pp. 2432–2447.

[13] Nayfeh, A. H. and Saric, W. S., "Non-Linear Stability of a Liquid Film Interacting with a Supersonic Stream," Research Rept. SC-RR-710042, 1971, Sandia Corp., Albuquerque, N. Mex.

[14] Nayfeh, A. H. and Saric, W. S., "Stability of a Liquid Film," *AIAA Journal*, Vol. 9, No. 4, April 1971, pp. 750–752.

[15] Miles, J. W., "The Hydrodynamic Stability of a Thin Film of Liquid in Uniform Shearing Motion," *Journal of Fluid Mechanics*, Vol. 8, 1960, pp. 593–610.

[16] Hanratty, T. J. and Engen, J. M., "Interaction Between a Turbulent Air Stream over a Moving Water Surface," *American Institute of Chemical Engineers Journal*, Vol. 3, 1957, pp. 299–310.

[17] van Rossum, J. J., "Experimental Investigation of Horizontal Liquid Film," *Chemical Engineering Science*, Vol. 11, 1959, pp. 35–42.

[18] Cohen, L. S. and Hanratty, T. J., "Generation of Waves in the Concurrent Flow of Air and a Liquid," *American Institute of Chemical Engineers Journal*, Vol. 31, 1968, pp. 467, 479.

[19] Cohen, L. S. and Hanratty, T. J., "Effect of Waves at a Gas-Liquid Interface on a Turbulent Air Flow," *Journal of Fluid Mechanics*, Vol. 31, 1968, pp. 467–479.

[20] Plate, E. J., Chang, P. C., and Hidy, G. M., "Experiments on the Generation of Small Water Waves by Wind," *Journal of Fluid Mechanics*, Vol. 35, 1969, pp. 625–656.

[21] Kendall, R. M. and Bartlett, E. P., "Nonsimilar Solution of the Multicomponent Laminar Boundary Layer by an Integral-Matrix Method," *AIAA Journal*, Vol. 6, No. 6, June 1968, pp. 1089–1097.

[22] Grose, R. G. and Kendall, R. M., "The Homogeneous BLIMP with Liquid Layer Option—User's Guide," Rept. 70-3, Feb. 1970, Aerotherm Corp., Mountain View, Calif.

[23] Pate, S. R., "Measurements and Correlations of Transition Reynolds Numbers on Sharp Slender Cones at High Speeds," AEDC-TR-69-172, Dec. 1969, Arnold Engineering Development Center, Tullahoma, Tenn.

[24] Hendry, J. P., "Boundary-Layer Transition Correlation for Sharp Slender Cones," *Journal of Spacecraft and Rockets*, Vol. 3, No. 3, March 1966, pp. 426–427.

[25] Muir, J. F. and Trujillo, A. A., "Experimental Investigation of the Effects of Nose Bluntness, Free-Stream Unit Reynolds Number, and Angle of Attack on Boundary Layer Transition at a Mach Number of 6," Research Rept. SC-RR-710046, 1971, Sandia Corp., Albuquerque, N. Mex.

[26] Stetson, K. F. and Rushton, G. H., "Shock Tunnel Investigation of Boundary-Layer Transition at $M = 5.5$," *AIAA Journal*, Vol. 5, No. 5, May 1967, pp. 899–906.

[27] Softly, E. J., "Boundary Layer Transition on Hypersonic Blunt Slender Cones," AIAA Paper 69-705, San Francisco, 1969.

[28] Craik, A. D. D., *Wind-Generated Waves in Liquid Films*, Ph.D. dissertation, 1965, Univ. of Cambridge.

[29] Saric, W. S. and Gibbons, R. S., "Stability of Axisymmetric Liquid Films," Research Rept. SC-RR-710019, 1971, Sandia Corp., Albuquerque, N. Mex.

AUGUST 1971 AIAA JOURNAL VOL. 9, NO. 8

An Analysis and Application of the Time-Dependent Turbulent Boundary-Layer Equations

HENRY McDONALD* AND STEPHEN J. SHAMROTH†
United Aircraft Research Laboratories, East Hartford, Conn.

The momentum and kinetic energy integral equations are derived for a compressible two-dimensional turbulent boundary layer with time-dependent mean velocity and density fields. The integral equations are used in conjunction with an assumed velocity profile family to predict the effect of small time-varying disturbances in the inviscid flow upon the behavior of a flat plate turbulent boundary layer. The prediction procedure is also used to investigate the possibility of dynamic coupling between small time-dependent disturbances in the inviscid flowfield and the resulting induced fluctuations arising from boundary-layer displacement effects. When applied to the flowfield resulting from a shock wave–boundary-layer interaction, the analysis predicts that certain disturbances couple with the boundary layer in an unstable manner and, thus, the analysis offers an explanation for an instability observed to occur in certain shock wave–boundary-layer interaction flowfields.

Nomenclature

C_f = skin-friction coefficient
H = shape factor
L = dissipation length
l = mixing length
M = Mach number
p = pressure
q = turbulence intensity
$T_{\text{ad wall}}$ = adiabatic wall temperature
T_{wall} = wall temperature
t = time
u = streamwise velocity
u_c = convection velocity
u_τ = friction velocity
u^* = Van Driest velocity
v = transverse velocity
x = streamwise coordinate
y = transverse coordinate
δ = boundary-layer thickness
δ^* = displacement thickness
γ = specific heat ratio
θ = momentum thickness
θ_E = kinetic energy thickness
θ_e = outer edge flow angle
θ_ρ = integral quantity defined by Eq. (12)
λ = disturbance wavelength
ρ = density
τ = shear stress
ω = disturbance frequency

Subscripts

e = quantity evaluated at outer edge of boundary layer
u = integral evaluated at constant density
w = quantity evaluated at wall

Received May 7, 1970; revision received December 14, 1970. This investigation was sponsored in part by Pratt and Whitney Aircraft.

* Supervisor, Theoretical Gas Dynamics Group.

† Research Engineer, Theoretical Gas Dynamics Group. Associate Member AIAA.

Superscripts

$\bar{\ }, \langle\ \rangle$ = average quantity
$'$ = fluctuating quantity

Introduction

UNTIL recently, analytical predictions of turbulent boundary-layer behavior were obtained almost solely from solutions of the boundary-layer integral equations in which the flow was assumed to be incompressible, steady on the average, and the turbulence was assumed to be in structural equilibrium.[1,2] In recent years the accessibility of high-speed computers has led to analyses of turbulent boundary layers based upon the finite difference solution of the partial differential equations of the mean motion, which include the effects of compressibility, wall heat transfer, and turbulence history.[3-6] However, to date, little progress has been made in relieving the assumption that the mean flow is steady on the average. Although the neglect of unsteady (in some average sense) phenomena is valid in a large number of cases of practical interest, several important cases exist in which the mean flow is known to contain large-amplitude, time-dependent oscillations. For example, a boundary layer developing on a stationary vane located behind a moving blade in a compressor or turbine is subjected to large-scale, time-dependent fluctuations in the inviscid flowfield. Time-dependent boundary layers also play an important role in the aerodynamic performance of helicopter rotor blades,[7] particularly during dynamic stall and, as a final example, in shock wave–boundary-layer interactions where under certain conditions, large-amplitude, time-dependent oscillations may appear in the interaction flowfield resulting in aerodynamic buffeting and structural fatigue.[8]

Although a modest effort has been undertaken to predict the behavior of unsteady laminar boundary layers, most of these analyses, as reviewed by Stewartson,[9] are limited by assumptions made in the form of the time-dependent portion of the flow or in the flow geometry. More recent laminar analyses of a more general nature have been carried out by McCroskey and Dwyer[7] and Presz and Heiser.[10] In contrast to the modest effort made in analyzing unsteady laminar boundary layers, little attempt has been made to investigate turbulent boundary layers whose mean flow is, in some average sense, time-dependent. Experimental investigations of time-dependent, turbulent boundary layers have been carried out by Karlsson[11] and Miller,[12] both of whom investigated flat plate incompressible turbulent boundary layers subjected to disturbances that vary sinusoidally with time. Measurements were made of both the streamwise velocity and the streamwise component of the turbulent intensity. To the authors' best knowledge, to date, no significant analytical investigations of time-dependent turbulent boundary layers have been carried out.

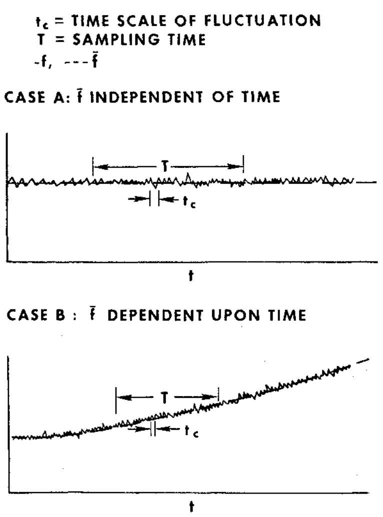

Fig. 1 Sketch for temporal average definition.

The preceding discussion clearly indicates that a practical need exists for developing more general techniques capable of predicting the behavior of both laminar and turbulent unsteady boundary layers. Such a calculation technique could be based upon either a numerical solution of the time-dependent boundary-layer equations of mean motion or upon the solution of a set of moment-of-momentum integral equations derived from the same equations of mean motion. Of these two types of solutions, numerical solutions of the partial differential equations contain the least and most easily isolated assumptions; however, they are also more time-consuming. With the advent of modern high-speed digital computers, numerical solutions of the steady-state boundary-layer equations are receiving more emphasis than integral solutions of these equations. However, when the flowfield is unsteady, a complete spatial solution of the boundary-layer equations must be found at each time step; and, since a number of time steps are required, the reduction in the number of approximations obtained by solving the original set of partial differential equations rather than a set of moment-of-momentum integral equations did not seem to be justified for the present initial study when weighed against both the computer running time and program development time. Consequently, in the present paper, a set of integral equations for the compressible boundary layer whose mean flow is time-dependent are derived. These equations are then used to calculate the properties of a time-dependent compressible turbulent boundary layer and to investigate the effect of small disturbances upon the flowfield resulting from a shock wave–boundary-layer interaction.

Description of the Analysis

Summary of the Solution Procedure

The present analysis is based upon a solution of the time-dependent integral turbulent boundary-layer equations of mean motion. As in most integral solutions of the boundary-layer equations, it is necessary to assume a velocity profile family and, for this purpose, the two-parameter velocity profile family of Coles,[13] as modified for compressible flow by Maise and McDonald,[14] is chosen. The boundary-layer behavior is predicted from a simultaneous solution of the time-dependent momentum integral equation and the time-dependent kinetic energy integral equation. The solutions are advanced in time using a predictor-corrector scheme to evaluate the time derivatives. At any time-step t_n the solution is obtained by first assuming values for all time derivatives appearing in the integral equations. When values are assumed for the time derivatives, the integral equations become ordinary differential equations with the streamwise coordinate as the independent variable and are solved numerically in the usual manner. The solution thus obtained gives provisional values of the velocity profile parameters at time t_n; and in order to ascertain the validity of the assumed time derivatives, finite differences are calculated from the provisional solution at t_n and the known solution at t_{n-1}. If both the assumed and calculated time derivatives agree within a predetermined tolerance, the behavior at $t = t_n$ has been predicted; if not, a new set of time derivatives is assumed and the calculation is repeated.

Derivation of the Integral Equations

The derivations of the unsteady momentum integral and kinetic energy integral equations are analogous to the derivations of the steady-state integral equations that may be found in most standard texts on boundary-layer theory (e.g., Ref. 15). All integral moment-of-momentum equations are derived from the equation of continuity, which may be written as

$$\partial\rho/\partial t + \partial\rho u/\partial x + \partial\rho v/\partial y = 0 \tag{1}$$

and the boundary-layer approximation to the streamwise momentum equation, which may be written as

$$\rho\frac{\partial u}{\partial t} + \rho u\frac{\partial u}{\partial x} + \rho v\frac{\partial u}{\partial y} = -\frac{\partial p}{\partial x} + \frac{\partial\tau}{\partial y} \tag{2}$$

If the flow is laminar, Eqs. (1) and (2) may be used as they appear. When the flow is turbulent, Eqs. (1) and (2) are quite intractable and the usual turbulent time-averaging procedure must be carried out. The question of defining the correct procedure by which averaging should be performed in a time-dependent mean flow is not answered simply; however, at this juncture a few comments are in order. If the averaging is done over an ensemble, then conceptually no problem arises either for steady or unsteady mean flow. However, an ensemble average is unsuitable both for interpreting experimental data and for giving clear physical significance to averaged quantities, and, therefore, for both purposes an alternative method of averaging will now be defined.

The usual averaging procedure is carried out with respect to time at a fixed point in space. Thus, if T is a time interval much larger than the characteristic time scale associated with the fluctuations in a quantity $f(x,y,z,t)$ then the average value of f at a given point is defined as

$$\bar{f}(x,y,z,t) = \frac{1}{T}\int_{t-T/2}^{t+T/2} f(x,y,z,t)dt \tag{3}$$

If $\bar{f}$ is independent of the sample time T and physical time t, the mean value is said to be independent of time as shown in Fig. 1a. However, it is possible to have a temporal variation in $\bar{f}$ with typical time scale T_1, sensibly independent of the sample time T if T_1 is much larger than the sample time T. Thus, if a time trace of a typical turbulent flow variable contains an easily filtered, very low frequency component, it is possible to average in the manner defined by Eq. (3) and so obtain a time-dependent mean variable as shown in Fig. 1b. In certain circumstances, such as when the mean quantity is a simple harmonic, it makes sense to filter out the harmonic prior to averaging. In the general case, however, the mean quantity is an arbitrary function of time, and consequently the simplified case is quite limited and will not be considered further in the present study. If the usual notation is used, in which overbars indicate average quantities and primes indicate fluctuating quantities, the time-averaged compressible turbulent boundary-layer equations become, in accordance with Eq. (3) (see, for instance, Schubauer and Tchen[16]),

$$\partial\bar{\rho}/\partial t + \partial\bar{\rho}\bar{u}/\partial x + \partial\langle\rho v\rangle/\partial y = 0 \tag{4}$$

$$\bar{\rho}\frac{\partial\bar{u}}{\partial t} + \bar{\rho}\bar{u}\frac{\partial\bar{u}}{\partial x} + \langle\rho v\rangle\frac{\partial\bar{u}}{\partial y} = -\frac{\partial\bar{p}}{\partial x} + \frac{\partial}{\partial y}\left(\bar{\mu}\frac{\partial\bar{u}}{\partial y} - \bar{\rho}\langle u'v'\rangle\right) \tag{5}$$

and

$$\tau = \bar{\mu}(\partial\bar{u}/\partial y) - \bar{\rho}\langle u'v'\rangle \tag{6}$$

$$\langle\rho v\rangle = \langle(\bar{\rho} + \rho')(\bar{v} + v')\rangle \tag{7}$$

In both laminar and turbulent flow it is usual to obtain ρv and $\langle\rho v\rangle$ from the continuity equations, Eqs. (1) and (4), respectively. If $\langle\rho v\rangle$ is obtained from the continuity equation and inserted into the appropriate streamwise momentum equation, then the laminar and turbulent streamwise momentum equations are formally identical except for the appropriate overbars. Since the momentum integral equations are derived from the full set of partial differential equations with ρv or $\langle\rho v\rangle$ eliminated precisely in this manner, it is permissible to drop the overbars and to consider the subsequent momentum integral equations as being valid for either laminar or turbulent flow with, of course, the proviso that in turbulent flow the appropriate overbars are implied.

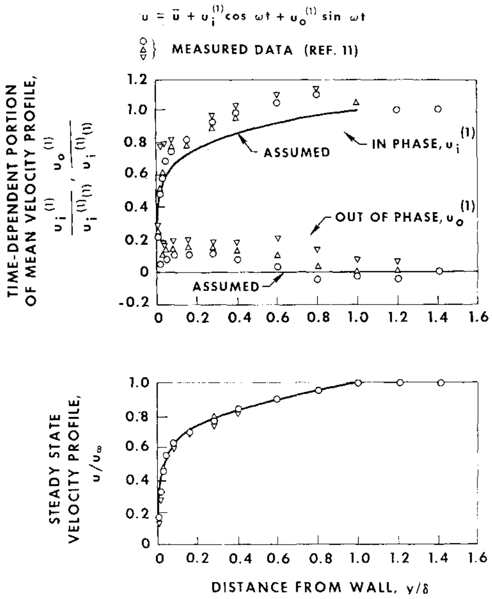

Fig. 2 A comparison between assumed and measured velocity profile.

Before proceeding further, it is convenient to express the streamwise pressure gradient, $\partial p/\partial x$, in terms of the external velocity and density distributions by examining the momentum equation at the outer edge of the boundary layer where the shear stress and transverse velocity gradients are negligible; the resulting expression for the streamwise pressure gradient is

$$\rho_e(\partial u_e/\partial t) + \rho_e u_e(\partial u_e/\partial x) = -\partial p/\partial x \tag{8}$$

It is now possible to derive the momentum integral equation for either laminar or turbulent flow by integrating Eq. (2) between limits $y = 0$ and $y = \delta$, and using Eqs. (1) and (8) to eliminate the explicit appearance of ρv and $\partial p/\partial x$. After some algebraic manipulation, the result is

$$\frac{\partial\theta}{\partial x} + \frac{\theta}{u_e}\frac{\partial u_e}{\partial x}(2 + H) + \frac{\theta}{\rho_e}\frac{\partial\rho_e}{\partial x} + \frac{1}{u_e}\frac{\partial\delta^*}{\partial t} + \frac{\delta^*}{u_e^2}\frac{\partial u_e}{\partial t} + \frac{\delta^*}{\rho_e u_e}\frac{\partial\rho_e}{\partial t} - \frac{1}{\rho_e u_e}\frac{\partial\rho_e}{\partial t}\theta_\rho - \frac{1}{u_e}\frac{\partial\theta_\rho}{\partial t} = \frac{C_f}{2} \tag{9}$$

where

$$\theta = \int_0^\delta \frac{\rho u}{\rho_e u_e}\left(1 - \frac{u}{u_e}\right)dy \tag{10}$$

$$\delta^* = \int_0^\delta\left(1 - \frac{\rho u}{\rho_e u_e}\right)dy \tag{11}$$

$$\theta_\rho = \int_0^\delta\left(1 - \frac{\rho}{\rho_e}\right)dy \tag{12}$$

$$C_f = \tau_w/\tfrac{1}{2}\rho_e u_e^2 \tag{13}$$

and H is the shape factor given by δ^*/θ. In Eqs. (9–13) the subscript e indicates that the subscripted quantity is evaluated at the outer edge of the boundary layer, and the subscript w indicates that the subscripted quantity is evaluated at the wall. Equation (9) is the momentum integral equation for a time-dependent compressible boundary layer.

The kinetic energy integral equation is obtained by multiplying the streamwise momentum equation by u, integrating the result between the limits of $y = 0$ and $y = \delta$, and utilizing the continuity equation to eliminate the explicit appearance of the transverse velocity v. Further arrangement eventually

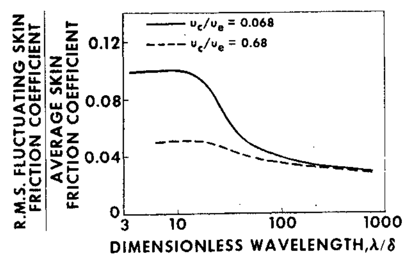

Fig. 3 Variation of fluctuating component of skin-friction coefficient with disturbance wavelength.

leads to the equation

$$\frac{\partial \theta_E}{\partial x} + 3\frac{\theta_E}{u_e}\frac{\partial u_e}{\partial x} + \frac{2}{u_e}\frac{\partial u_e}{\partial x}(\delta^* - \delta_u^*) + \frac{\theta_E}{\rho_e}\frac{\partial \rho_e}{\partial x} + \frac{1}{u_e}\frac{\partial}{\partial t}(\delta^* + \theta) + \frac{\theta}{\rho_e u_e^3}\frac{\partial \rho_e u_e^2}{\partial t} + \frac{2}{u_e^2}\frac{\partial u_e}{\partial t}(\delta^* - \delta_u^*) - \frac{1}{u_e}\frac{\partial \theta_\rho}{\partial t} - \frac{1}{\rho_e u_e}\frac{\partial \rho_e}{\partial t}\theta_\rho + \frac{\delta^*}{\rho_e u_e}\frac{\partial \rho_e}{\partial t} = \frac{2}{\rho_e u_e^3}\int_0^\delta \tau \frac{\partial u}{\partial y}dy \quad (14)$$

where

$$\delta_u^* = \int_0^\delta \left(1 - \frac{u}{u_e}\right)dy \quad (15)$$

and

$$\theta_E = \int_0^\delta \frac{\rho u}{\rho_e u_e}\left[1 - \left(\frac{u}{u_e}\right)^2\right]dy \quad (16)$$

Velocity Profile Family

The momentum and kinetic energy integral equations represent a pair of simultaneous differential equations which, upon specification of an inviscid flowfield and initial conditions, lead to a prediction of the boundary-layer development. However, as in the case of most steady-state integral boundary-layer analyses, the number of unknown integral thicknesses appearing in the governing equations, Eqs. (9) and (14), exceeds the number of governing equations. As in steady-state integral boundary-layer theory, a solution is obtained by specification of a velocity profile family, a velocity-temperature relationship, and a velocity-Reynolds stress relationship. The profile family chosen in the present analysis is the two-parameter profile family of Coles,[13] as modified for compressible flow by Maise and McDonald.[14] In Ref. 13 Coles has shown that this velocity profile representation is quite accurate in incompressible flows having arbitrary, modest pressure gradients. This representation has been extended to compressible flows by Maise and McDonald,[14] who suggest replacing the physical streamwise velocity u in Coles' law of the wall-law of the wake formulation by the

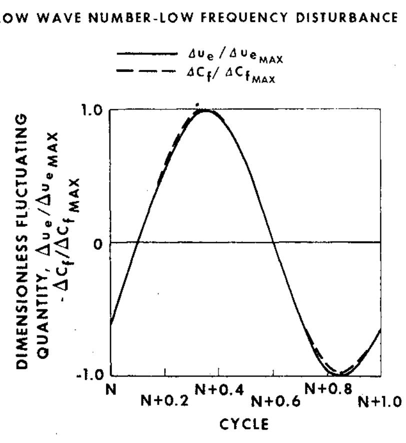

Fig. 4 Phase relation for traveling sinusoidal disturbances.

Van Driest velocity u^*. Following this suggestion, the velocity profile becomes

$$u^*/u_\tau = 1/\kappa \ln(yu_\tau/\nu) + C + \pi/\kappa w(y/\delta) \quad (17)$$

where w is Coles' universal wake function, κ and C are the usual law of the wall constants, π is the wake parameter (a function only of x), and u^* is the Van Driest velocity given by

$$u^* = (u_e/A)\sin^{-1}[\{2A^2(u/u_e) - B\}/(B^2 + 4A^2)^{1/2}] \quad (18)$$

where

$$A^2 = [(\gamma - 1)/2]M_e^2(T_e/T_w) \quad (19)$$

$$B = \{1 + [(\gamma - 1)/2]M_e^2\}(T_e/T_w) - 1 \quad (20)$$

In Ref. 14 Maise and McDonald have shown that Eq. (17) is a good representation of velocity profiles for compressible, constant pressure, turbulent boundary layers, and more recently, Mathews, Paynter, and Childs[17] have shown that Eq. (17) is a good representation of velocity profiles for compressible turbulent boundary layers subjected to modest streamwise pressure gradients.

In addition to being a good representation of steady-state turbulent boundary layers, Karlsson's data[11] leads one to suggest that Coles' profile might also be a good representation for time-dependent boundary layers. In his investigation, Karlsson subjected a flat plate boundary layer to an inviscid velocity distribution of the form

$$u_e(x,t) = \bar{u}_e(x) + u_{e_i}^{(1)}\cos\omega t \quad (21)$$

and then measured the streamwise velocity within the boundary layer. Expressing this velocity by

$$u(x,y,t) = \bar{u}(x,y) + u_i^{(1)}(x,y)\cos\omega t + u_0^{(1)}(x,y)\sin\omega t \quad (22)$$

Karlsson measured $\bar{u}$, $u_i^{(1)}$ and $u_0^{(1)}$. Obviously, at the edge of the boundary layer $u_{e_i}^{(1)}$ and $u_i^{(1)}$ are identical and $u_0^{(1)}$ is zero. In Fig. 2, Karlsson's data for $\bar{u}(x,y)$ is compared to Coles' profile. In constructing Coles' profile for this comparison, the skin-friction coefficient and momentum thickness were matched to Karlsson's data; the agreement is excellent. The fluctuating portion of the profile is also shown in Fig. 2. If the assumption that Coles' profile were correct at any instant of time were exact, the in-phase component of the fluctuating velocity $u_i^{(1)}$ would agree exactly with Coles' profile, and the out-of-phase component $u_0^{(1)}$ would be identically zero. Although the agreement is not exact, it is moderately good and, in view of the success of many steady-state integral methods which do not accurately represent the true velocity profile, Coles' profile should be adequate for obtaining reasonably accurate predictions of the time-dependent turbulent boundary-layer behavior.

In addition to assuming a velocity profile family, it is also necessary to either assume a temperature profile or a temperature-velocity relation. In the present analysis in which all boundary layers investigated are nearly adiabatic, the temperature and velocity are assumed to be related by

$$\frac{T}{T_e} = 1 + \frac{\gamma - 1}{2}M_e^2\left[1 - \left(\frac{u}{u_e}\right)^2\right] + \frac{T_{\text{wall}} - T_{\text{ad. wall}}}{T_e} \times \left[1 - \left(\frac{u}{u_e}\right)\right] \quad (23)$$

a relation which is known to be reasonably valid for nearly adiabatic boundary layers. Obviously, Coles' profile is not the sole profile which can be used in a time-dependent integral analysis. One possible alternative suitable for cases in which the inviscid flowfield is sinusoidal in time would assume that the instantaneous velocity profile could be represented by Eq. (22) where $u_i^{(1)}$ and $u_0^{(1)}$ were functions of time. In such a representation, Coles' profile still would be used to represent the mean velocity field $\bar{u}(x,y)$, and empirical expressions could be derived from Karlsson's data for $u_i^{(1)}$ and $u_0^{(1)}$. Although such a representation may represent the instantaneous velocity more accurately than Coles' profile, a representation based on Eq. (22) would require additional integral equations to determine the additional profile parameters. In view of these considerations and in view of the reasonable agreement of Coles' profile with Karlsson's data, the present investigation used Coles' profile to represent the instantaneous velocity profile.

Turbulence Model

In addition to hypothesizing a velocity profile family and a velocity-temperature relation, it is also necessary to hypothesize a model for the turbulent shear stress. In many cases, accurate predictions for turbulent shear flows can be obtained by hypothesizing the existence of an eddy viscosity or mixing length, the magnitude of which depends only upon local mean flow conditions; such a turbulence model is termed an equilibrium turbulence model. However, under certain conditions, experimental evidence clearly shows that the turbulent shear stress is strongly dependent upon the upstream history of the boundary layer (e.g., Ref. 18). In such cases a turbulence model based solely upon local mean conditions is not adequate, and a model including the effects of turbulence history, both temporal and spatial, should be used. At the present time several calculation procedures, such as those of Fish and McDonald[19] or Bradshaw and Ferris,[20] have been developed and successfully utilized to include the effect of spatial turbulence history. However, to date, no significant attempt has been made to include the effect of temporal turbulence history. A model including the effects of temporal turbulence history can be obtained from the turbulence kinetic energy equation which in its time-dependent form is written as

$$\underbrace{\frac{\partial}{\partial t}\left(\frac{1}{2}\,\bar{\rho}\langle q^2\rangle\right)}_{\text{time rate of change}} + \underbrace{\frac{\partial}{\partial x}\left(\frac{1}{2}\,\bar{\rho}\bar{u}\langle q^2\rangle\right) + \frac{\partial}{\partial y}\left(\frac{1}{2}\,\langle\rho v\rangle\langle q^2\rangle\right)}_{\text{advection (mean flow convection)}} =$$

$$\underbrace{-\bar{\rho}\langle u'v'\rangle\frac{\partial\bar{u}}{\partial y} - \langle\rho'u'\rangle\frac{\partial\bar{u}}{\partial t}}_{\text{production}} - \frac{\partial}{\partial y}\times$$

$$\underbrace{\left(\langle p'v'\rangle + \frac{1}{2}\,\bar{\rho}\langle q^2v'\rangle + \frac{1}{2}\,\langle\rho' q^2 v'\rangle\right)}_{\text{diffusion}}$$

$$\underbrace{-\bar{\rho}\epsilon}_{\text{dissipation}} \underbrace{- \bar{\rho}\left(\langle u'^2\rangle - \langle v'^2\rangle\right)\frac{\partial\bar{u}}{\partial x}}_{\text{normal stress term}} \qquad (24)$$

where $\langle q^2\rangle$, the turbulence intensity, is defined as

$$\langle q^2\rangle = \langle u'^2\rangle + \langle v'^2\rangle + \langle w'^2\rangle \qquad (25)$$

and ϵ represents the sum of the turbulent dissipation terms. Equation (24) can be solved either by extending the calculation procedure of Fish and McDonald[19] or that of Bradshaw and Ferris[20] to include time as an independent variable.

It follows from Eq. (24) that if both the time rate of change and the advection of turbulent intensity is negligible in comparison with the production of turbulence, then an equilibrium turbulence model would be a valid approximation. The requirements for negligible advection of turbulent intensity are discussed elsewhere (Refs. 5 and 6, for instance) and a simple order of magnitude analysis shows that the time rate of change of turbulent intensity would be negligible for typical frequencies ω_c where

$$\omega_c \ll u_e/\delta \qquad (26)$$

Since, in addition to the order of magnitude argument, experimental evidence (e.g., Ref. 21) indicates that the characteristic frequency of the energy containing portion of the turbulence is given approximately by u_e/δ, it was felt reasonable to limit the use of an equilibrium turbulence model to flows where the mean flow frequency was much less than u_e/δ. For the initial study reported in the present note, only mean flows satisfying Eq. (26) are investigated, and thus the turbulent shear stress is calculated using an equilibrium mixing length model in which the mixing length l is given by

$$l/\delta = 0.09\tanh(\kappa y/0.09\delta) \qquad (27)$$

and the turbulent shear stress is then given by

$$\tau/\rho = l^2|\partial u/\partial y|\partial u/\partial y \qquad (28)$$

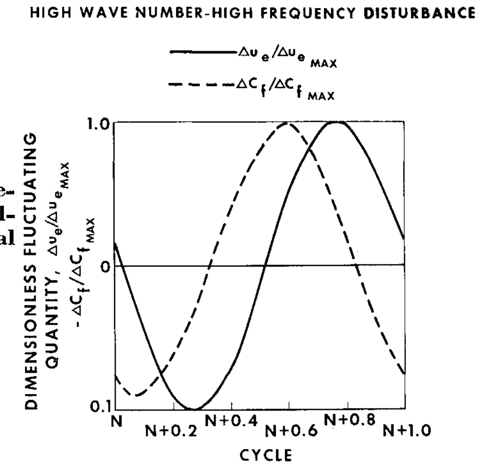

Fig. 5 Phase relation for traveling sinusoidal disturbances.

Some Computed Results for the Unsteady Flat Plate Boundary Layer

A simple example of a time-dependent flow problem is that of a boundary layer developing on a flat plate subjected to traveling disturbances in the inviscid flowfield. The computed effects on the boundary layer of a traveling sinusoidal disturbance superimposed upon an inviscid flowfield having a constant Mach number, $M_e = 1.59$, is presented in Figs. 3–5. In these calculations the inviscid velocity distribution, including the disturbance, is assumed to be

$$u_e = u_b[1 + 0.01\sin(2\pi x/\lambda + \omega t)] \qquad (29)$$

and the freestream density distribution is assumed to be

$$\rho_e = \rho_b[1 + 0.01\sin(2\pi x/\lambda + \omega t + \pi)] \qquad (30)$$

In Eqs. (29) and (30) the subscript b indicates the undisturbed quantity. It should be noted that the assumed disturbance is one of zero first-order mass flow. When the inviscid flowfield velocity and density distributions are specified by Eqs. (29) and (30), the inviscid static pressure distribution is calculated from

$$\partial p_e/\partial x = -\rho_e(\partial u_e/\partial t) - \rho_e u_e(\partial u_e/\partial x) \qquad (31)$$

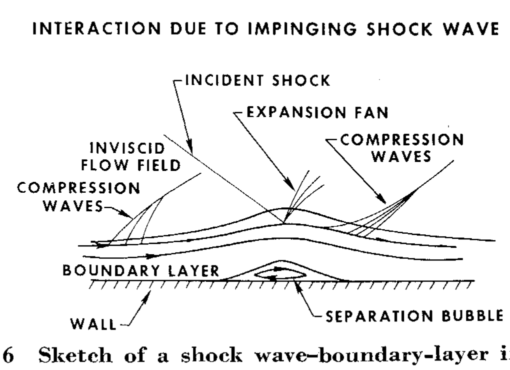

Fig. 6 Sketch of a shock wave–boundary-layer interaction.

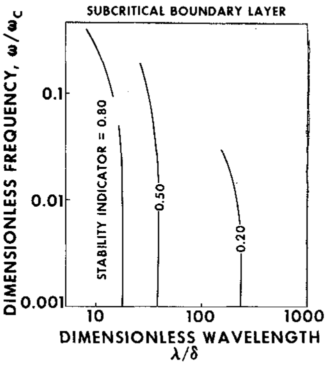

Fig. 7 Stability diagram for traveling sinusoidal wave.

and the inviscid static temperature distribution is then determined from the equation of state. In all calculations presented in this paper, the initial conditions required for the boundary-layer calculation are obtained by assuming that the friction velocity u_τ and Coles' wake parameter π are constant at an initial streamwise station.

In Fig. 3 the root-mean-square value of the fluctuating skin-friction coefficient is plotted as a function of dimensionless wavelength for two different disturbance convection velocities. For the purpose of this paper a fluctuating quantity is defined as the difference between the quantity calculated when a disturbance is present in the inviscid flowfield and the quantity calculated for the undisturbed inviscid flowfield at the same streamwise station. It should be noted that if the convection velocity of the disturbance is held constant, a decrease in disturbance wavelength is accompanied by an increase in disturbance frequency and, thus, Fig. 3 also represents the variation of root-mean-square fluctuating skin friction with disturbance frequency. The results of Fig. 3 indicate that at relatively large disturbance wavelengths a decrease in disturbance wavelength is accompanied by an increase in the root-mean-square fluctuating skin friction. Since a decrease in wavelength for the assumed disturbance results in an increase in the disturbance pressure gradient, the accompanying increase in root-mean-square fluctuating quantities is to be expected. However, as the disturbance wavelength decreases, changes in the disturbance pressure gradient become more and more rapid (or in other words second derivatives of the pressure become larger and larger), and at some wavelength inertial effects would be expected to prevent the boundary layer from responding to further decreases in disturbance wavelength. The present theory predicts this lack of response to occur at a disturbance wavelength approximately equal to ten boundary-layer thicknesses.

The phase relation between the fluctuating skin friction and the time-dependent fluctuating inviscid flow disturbance is shown in Figs. 4 and 5. In both figures results are presented at a given streamwise station over a time span equal to a disturbance period; in Fig. 4 typical results for a low wave number–low frequency disturbance indicate that the fluctuating skin friction is in phase with the inviscid flow disturbance and varies sinusoidally with time. The result presented in Fig. 4 is to be expected since if the disturbance is of low frequency and low wave number, the boundary layer can adjust to the instantaneous inviscid flow conditions. However, if the disturbance is of high frequency and high wave number, the boundary layer is no longer able to adjust to the instantaneous freestream conditions and phase discrepancies as well as distortions in wave form appear as shown in Fig. 5. As predicted for laminar boundary layers by Lighthill[22] and Lin,[23] Fig. 5 shows that the fluctuating skin friction anticipates the inviscid flow disturbances. The predictions of Lighthill and Lin were based upon the concept that the low inertia of the flow in the inner portion of the boundary layer results in the skin friction anticipating the inviscid flow disturbance. Since the inner portion of a turbulent boundary layer is also a region of relatively low inertia, the same phase difference should occur in fluctuating turbulent boundary layers and, thus, the results appearing in Fig. 5 are to be expected.

Application to the Problem of an Unsteady Shock Wave–Boundary-Layer Interaction

One important example of a time-dependent flow problem mentioned in the Introduction is that of a shock wave–boundary-layer interaction. A sketch of a typical interaction flowfield is shown in Fig. 6. The shock wave–boundary-layer interaction flowfield belongs to a class of problems known as strong-interaction problems in which the usual boundary-layer assumption that the streamwise pressure distribution along a surface is independent of the boundary layer developing on the surface is known to be invalid. Hence, the usual boundary-layer technique of obtaining the streamwise pressure distribution from an analysis which ignores the existence of a boundary layer is incorrect; in fact, the pressure distribution must either be obtained from experimental data or must be calculated in a manner which accounts for the mutual interaction between the inviscid flowfield and the boundary layer. The problem of calculating a strong interaction flowfield in a manner which accounts for this mutual interaction is quite formidable and a full discussion of the problems associated with such procedures may be found in Refs. 24–27. In the present application of the time-dependent boundary-layer equations to the unsteady shock wave–boundary-layer interaction problem, a steady-state streamwise pressure distribution through the interaction region is required. This distribution is obtained from experimental data.

Although most analyses of the interaction flowfield assume that the interaction is a steady-state phenomena, experimental evidence clearly shows that interaction flowfields do contain time-dependent disturbances. If the magnitude of these disturbances remains small, the steady-state assumption is a good one; however, under certain conditions these disturbances are amplified through the dynamics of the interaction and result in a flowfield containing large-amplitude, time-dependent disturbances. The appearance of such large-amplitude, time-dependent disturbances has been observed by Alford and Taylor[8] in the case of a high area ratio nozzle operated at pressure ratios not great enough to allow full expansion of the exhaust gas to the nozzle exit area. Since these large-amplitude disturbances can lead to severe aerodynamic buffeting and structural fatigue, it is imperative that conditions under which they appear be avoided. The following portion of the present paper describes a preliminary analysis motivated by the necessity for predicting the conditions under which these large-amplitude, time-dependent disturbances can appear in a shock wave–boundary-layer interaction flowfield.

The only previous attempt to analyze the shock wave–boundary-layer interaction stability problem, which appears in the open literature, was carried out by Trilling,[28] who hypothesized a semiempirical stability model. In addition to its empirical nature, Trilling's analysis contains two restrictive assumptions: the boundary layer is assumed to separate from the wall during the interaction, and the boundary layer is assumed to reattach to the wall at some downstream station. In contrast to laminar boundary layers which almost always separate while interacting with a shock wave, turbulent boundary layers can remain attached throughout the interaction process. Furthermore, in the common interaction occurring in an exhaust nozzle, the boundary layer after separating does not reattach to the wall; instead, it passes through the nozzle exit plane as a free shear layer. Thus both the empirical nature of Trilling's analysis and its constraining assumptions seem to preclude a direct extension of this analysis to the case of a general shock wave–turbulent boundary-layer interaction.

Stability Analysis

In the present analysis a steady-state streamwise static pressure distribution in the vicinity of a shock wave–boundary-layer interaction is assumed from experimental data and then used as input for the previously described integral boundary-layer calculation procedure. For the purpose of this discussion the streamwise velocity at the outer edge of the boundary layer for the case of the steady-state interaction is termed $u_b(x)$. The integral boundary-layer calculation procedure then predicts the steady-state boundary layer developing under the assumed pressure distribution. Among other quantities predicted is the flow angle at the outer edge of the boundary layer $\theta_b(x)$, which is also known as the inviscid flow angle. After the steady-state boundary layer is calculated, a small time-dependent disturbance is superimposed upon the steady-state inviscid flowfield; the resulting streamwise velocity distribution is termed $u_e(x,t)$, where $u_e(x,t)$ is the sum of the steady-state distribution $u_b(x)$ and a disturbance distribution $u_d(x,t)$. This disturbed inviscid flowfield is input into the time-dependent integral boundary-layer calculation procedure which predicts, among other quantities, the time-dependent inviscid flow angle $\theta_e(x,t)$. The two flow angles $\theta_e(x,t)$ and $\theta_b(x)$ serve to define a disturbance flow angle $\theta_d(x,t)$. If the inviscid flowfield is governed by the Prandtl-Meyer relation, the change in flow angle

$$\theta_d(x,t) = \theta_e(x,t) - \theta_b(x) \qquad (32)$$

induces a change in the inviscid flowfield velocity component parallel to the boundary given by

$$\Delta u_i = -u_b\theta_d[\tan\theta_b + 1/(M_e^2 - 1)^{1/2}] \qquad (33)$$

It is important to understand that Δu_i is the change in velocity that would be induced in the outer inviscid flow if the boundary-layer inviscid flow angle underwent a change θ_d. The stability of the boundary layer at a specific time $t = t_1$ and at a specific streamwise station $x = x_1$ is now determined by comparing u_d and Δu_i. A stability factor is defined by the equation

$$\text{s.f.}(x,t) = (u_d - \Delta u_i)/u_d \qquad (34)$$

If s.f.$(x,t) > 1$, u_d and Δu_i are of the opposite sign and the flow is stable. If $0 <$ s.f. < 1, u_d and Δu_i are of the same sign but $|\Delta u_i| < |u_d|$ and the flow is again stable. If s.f. < 0, u_d and Δu_i are of the same sign and $|\Delta u_i| > |u_d|$. In this case the flow is unstable. In summary

$$\text{s.f.} > 0 \text{ stable} \qquad (35)$$

$$\text{s.f.} < 0 \text{ unstable} \qquad (36)$$

The stability factor predicts stability at a given streamwise station at a given time; however, a more general concept is required to predict the stability of a flow domain over a finite time interval. For this purpose the stability indicator is defined by the equation

$$\text{s.i.} = \frac{1}{(x_2 - x_1)T}\int_0^T\int_{x_1}^{x_2} F dx dt \qquad (37)$$

where

$$F = +1 \text{ if s.f.} > 0 \qquad (38)$$

$$F = -1 \text{ if s.f.} < 0 \qquad (39)$$

where x_1 is a streamwise location slightly upstream of the domain of interest, x_2 is a streamwise location slightly downstream of the domain of interest, and T is the time interval. For the purpose of the present stability investigation, the domain of interest is the streamwise extent of the shock wave–boundary-layer interaction and the time interval T is a disturbance period. By definition, the stability indicator may take on values in the range of -1 to $+1$; negative values indicate that the flow is relatively unstable, and positive values indicate that the flow is relatively stable to the imposed disturbance.

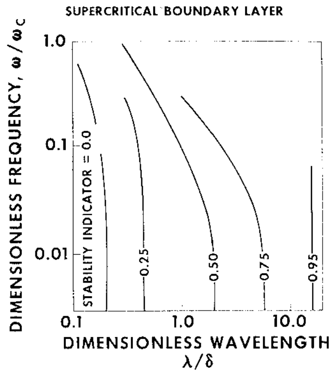

Fig. 8 Stability diagram for traveling sinusoidal wave.

Obviously, the present analysis has several shortcomings which must be improved upon before the results of a stability analysis can be accepted with quantitative confidence. Perhaps the most serious shortcoming is the neglect of normal pressure gradients, which are known to play an important role in the mutual interaction between the boundary layer and the outer inviscid flow (e.g., see Ref. 25). Nevertheless, the present preliminary analysis does yield qualitative information concerning the stability problem and may be regarded as a first step in a more complex but more rigorous stability analysis.

Results of the Stability Calculation

Stability calculations were carried out for two different shock wave–boundary-layer interaction flowfields. In the first calculation the boundary layer was subcritical and in the second calculation the boundary layer was supercritical. The terms subcritical and supercritical refer to the manner in which the quasi-steady boundary-layer outer edge flow angle responds to small changes in local streamwise pressure gradient. If a positive pressure gradient makes a positive contribution to the inviscid flow angle, the flow is termed subcritical, and if it makes a negative contribution to the inviscid flow angle, the flow is termed supercritical. By analogy with one-dimensional compressible gas dynamics, subcritical boundary layers may be thought of as subsonic in a mean sense and supercritical boundary layers as supersonic in a mean sense. This concept of criticality has been put into quantitative terms by Weinbaum and Garvine.[26] According to steady-state strong-interaction theory, the predicted behavior of subcritical boundary layers is distinctly different from the predicted behavior of supercritical boundary layers[25–27] and the present study shows these differences to carry over to predictions of stability of an interaction flowfield to small disturbances.

The first stability calculation was carried out for what turned out to be a subcritical shock wave–boundary-layer interaction in which the freestream Mach number was assumed to decrease from an initial value of 1.49 to a final value of 1.10. In this interaction the streamwise pressure distribution was taken from the work of Gadd et al.[29] for a boundary layer that remained attached throughout the interaction. The average criticality of the boundary layer in the region of the interaction was determined by an application of Weinbaum's criterion,[26] which states that in the absence of normal pressure gradients, a boundary layer is subcritical if

$$\int_0^\delta \frac{1 - M^2}{M^2 dy} > 0$$

and supercritical if this integral is less than zero. The criticality was determined by solving the steady-state boundary-layer equations under the assumed pressure distribution and then evaluating Weinbaum's integral at each streamwise station. Although the boundary layer is initially supercritical, it becomes subcritical approximately one-fourth of the way through the interaction and then remains subcritical. Furthermore, the streamwise average value of

$$\int_0^\delta \frac{1 - M^2}{M^2 dy}$$

when taken over the region of increasing static pressure, is larger than zero; hence, the boundary layer, although initially supercritical, is subcritical on average. The interaction flowfield thus obtained was assumed to be subjected to a velocity and density disturbance given by Eqs. (29) and (30) and the stability of the interaction flowfield was predicted for disturbances of various wavelengths and frequencies.

The results of the stability calculation for a subcritical boundary layer are presented in Fig. 7, where it is shown that the subcritical boundary layer is relatively unstable to long wavelength disturbances and, furthermore, at a given wavelength, the flowfield becomes less stable as the disturbance frequency increases. The results of an identical investigation for a supercritical boundary layer are presented in Fig. 8. In the supercritical interaction, the upstream Mach number is 3.0 and the downstream Mach number is 2.7; again, the boundary layer remains attached throughout the interaction. In contrast to the subcritical interaction, the supercritical interaction is stable for large wavelength disturbances and becomes unstable as the disturbance wavelength decreases. Furthermore, while subcritical boundary layers become less stable as the frequency increases at a given wavelength, supercritical boundary layers show opposite behavior as they are less stable to low frequency disturbances than to high frequency disturbances at a given disturbance wavelength. It should be noted that the preceding calculations were carried out for specific steady-state pressure distributions; however, it is expected that qualitatively the difference in behavior between subcritical and supercritical boundary layers would be predicted regardless of the specific pressure distribution chosen.

Although the quantitative results presented in the stability diagrams should be viewed with caution due to the simplified boundary-layer model, the qualitative results do show that under certain conditions small disturbances in the inviscid flowfield can be amplified through the dynamics of the interaction and, thus, the results offer an explanation for the observed instability.

References

[1] Thompson, B. G. J., "A Critical Review of Existing Methods for Calculating the Turbulent Boundary Layer," R&M 3447, 1967, Aeronautical Research Council, London, Great Britain.

[2] Rotta, J. C., "Turbulent Boundary Layers in Incompressible Flow," *Progress in the Aeronautical Sciences*, Vol. 2, Macmillan, New York, 1962.

[3] Herring, H. J. and Mellor, G., "A Method of Calculating Compressible Turbulent Boundary Layers," CR-1144, Sept. 1968, NASA.

[4] McDonald, H., "An Assessment of Certain Procedures for Computing the Compressible Turbulent Boundary Layer Development," *Proceedings of the Symposium on Compressible Turbulent Boundary Layers*, NASA SP-216, Dec. 1968, pp. 181–229.

[5] Bradshaw, P., Ferris, D. H., and Atwell, N. P., "Calculation of Boundary Layer Development Using the Turbulent Kinetic Energy Equation," *Journal of Fluid Mechanics*, Vol. 28, Pt. 3, May 1967, pp. 593–616.

[6] McDonald, H. and Camarata, F. J., "An Extended Mixing Length Approach for Computing the Turbulent Boundary Layer Development," *Proceedings of the AFOSR-IFP-Stanford Conference on Computation of Turbulent Boundary Layers*, 1968, pp. 83–98.

[7] Dwyer, H. A. and McCroskey, W. J., "Crossflow and Unsteady Boundary-Layer Effects on Rotating Blades," *AIAA Journal*, to be published.

[8] Alford, J. S. and Taylor, R. P., "Aerodynamic Stability Considerations of High Pressure Ratio, Variable Geometry Jet Nozzles," *Journal of Aircraft*, Vol. 2, No. 4, July-Aug. 1965, pp. 308–311.

[9] Stewartson, K., "The Theory of Unsteady Laminar Boundary Layers," *Advances in Applied Mechanics*, Vol. 6, edited by H. L. Dryden and T. von Kármán, Academic Press, New York, 1962, pp. 1–37.

[10] Presz, W. M. and Heiser, W. H., "Unsteady Boundary Layer Analysis for Two-Dimensional Laminar Flow," *Zeitschrift fur Flugwissenschaften*, Vol. 16, No. 2, Feb. 1968, pp. 33–39.

[11] Karlsson, S. K. F., "An Unsteady Turbulent Boundary Layer," *Journal of Fluid Mechanics*, Vol. 5, Pt. 2, May 1959, pp. 622–636.

[12] Miller, J. A., "Heat Transfer in the Oscillating Turbulent Boundary Layer," *Journal of Engineering for Power*, Vol. 91, No. 4, Oct. 1969, pp. 239–244.

[13] Coles, D., "The Law of the Wake in the Turbulent Boundary Layer," *Journal of Fluid Mechanics*, Vol. 1, Pt. 2, July 1956, pp. 191–226.

[14] Maise, G. and McDonald, H., "Mixing Length and Kinematic Eddy Viscosity in a Compressible Boundary Layer," *AIAA Journal*, Vol. 6, No. 1, Jan. 1968, pp. 73–79.

[15] Schlichting, H., *Boundary Layer Theory*, 6th edition, McGraw-Hill, New York, 1968.

[16] Schubauer, G. B. and Tchen, C. M., *Turbulent Flow*, Princeton University Press, Princeton, N. J., 1961, Chap. 2.

[17] Mathews, D. C., Paynter, G. C., and Childs, M. E., "On the Use of Coles' Universal Wake Function for Compressible Turbulent Boundary Layers," *Journal of Aircraft*, Vol. 7, No. 2, March-April 1970, pp. 137–140.

[18] Mueller, T. M. and Robertson, J. M., "A Study of the Mean Motion and Turbulence Downstream of a Roughness Element," *Modern Development is Theoretical and Applied Mechanics*, Vol. 1, Plenum Press, New York, 1963.

[19] Fish, R. W. and McDonald, H., "Practical Calculations of Transitional Boundary Layers," UAR-H48, March 1969, United Aircraft Corp., East Hartford, Conn.

[20] Bradshaw, P. and Ferris, D. H., "Calculation of Boundary Layer Development Using the Turbulent Energy Equation, Part II, Compressible Flow on Adiabatic Walls," Aero. Rept. 1217, 1966, National Physics Lab., Great Britain.

[21] Bradshaw, P. and Ferris, D. H., "The Response of a Retarded Equilibrium Turbulent Boundary Layer to the Sudden Removal of Pressure Gradient," Aero. Rept. 1145, 1965, National Physics Lab., Great Britain.

[22] Lighthill, M. J., "The Response of Laminar Skin Friction and Heat Transfer to Fluctuations in the Stream Velocity," *Proceedings of the Royal Society, Ser. A*, Vol. A224, June 1954, pp. 1–23.

[23] Lin, C. C., "Motion in the Boundary Layer with a Rapidly Oscillating External Flow," *Proceedings of the Ninth Congress of Applied Mechanics*, Vol. 4, 1956, pp. 155–168.

[24] Lees, L. and Reeves, B. L., "Supersonic Separated and Reattaching Flows: I. General Theory and Application to Adiabatic Boundary-Layer/Shock-Wave Interactions," *AIAA Journal*, Vol. 2, No. 11, Nov. 1964, pp. 1907–1920.

[25] Shamroth, S. J. and McDonald, H., "A New Solution of the Turbulent Near-Wake Recompression Problem," AIAA Paper 70-228, New York, 1970.

[26] Weinbaum, S. and Garvine, R. W., "On the Two-Dimensional Viscous Counterpart of the One-Dimensional Sonic Throat," *Journal of Fluid Mechanics*, Vol. 39, Pt. 1, 1969, pp. 57–85.

[27] Klineberg, J. M. and Lees, L., "Theory of the Laminar Viscous-Inviscid Interaction in Supersonic Flow," *AIAA Journal*, Vol. 7, No. 12, Dec. 1969, pp. 2211–2221.

[28] Trilling, L., "Oscillating Shock Wave-Boundary Layer Interaction," *Journal of the Aeronautical Sciences*, Vol. 25, No. 5, May 1958, pp. 301–304.

[29] Gadd, G. E., Holder, D. W., and Regan, J. D., "An Experimental Investigation of the Interaction Between Shock Waves and Boundary Layers," *Proceedings of the Royal Society, Ser. A*, Vol. 226, 1954, pp. 227–253.